Articles

Impact of Proline Residues on Parvalbumin Stability†

Sayeh Agah, John D. Larson, and Michael T. Henzl*

Department of Biochemistry, University of Missouri−Columbia, Columbia, Missouri 65211

Received May 4, 2003; Revised Manuscript Received July 17, 2003

ABSTRACT: Despite its higher net charge and reduced opportunities for favorable tertiary interactions, Ca^{2+}-free rat β-parvalbumin is more stable than rat α-parvalbumin. Under conditions wherein α denatures at 45.8 °C, β denatures at 53.6°. The homologous chicken β isoform known as CPV3 also exhibits heightened stability—prompting an inquiry into the stabilizing influence of Pro-21 and Pro-26. Individual P21A and P26A mutations lower the T_m of rat β by 3.2°, decreasing conformational stability by 0.74 kcal/mol. Simultaneous replacement of Pro-21 and Pro-26 essentially abolishes the excess stability ($\Delta T_m = -7.6°$; $\Delta\Delta G_{conf} = -1.77$ kcal/mol). Significantly, the P21A/P26A variant displays Ca^{2+} affinity virtually indistinguishable from wild-type β, implying that structural alterations in the AB domain do not necessarily influence the divalent ion affinity of the CD-EF domain. The consequences of introducing proline at positions 21 and 26 in rat α were also examined. Whereas the H26P mutation raises the T_m by 5.6° ($\Delta\Delta G_{conf} = 1.25$ kcal/mol), A21P lowers the T_m by 8.5° ($\Delta\Delta G_{conf} = -1.9$ kcal/mol). Replacement of Ala-21 by proline in an α AB/β CD-EF chimera increases the T_m by 5.8° ($\Delta\Delta G_{conf} = 0.95$ kcal/mol), implying that the destabilization of α by Pro-21 results from steric conflict with a residue in the CD-EF domain. Consistent with that hypothesis, the K80S mutation markedly stabilizes α A21P, yielding a protein with a T_m 2.0° higher than wild-type α. The observed differences in stability resulting from proline addition/removal are largely consistent with alterations in main-chain and side-chain conformational entropy.

The EF-hand family—the largest class of intracellular Ca^{2+}-binding proteins—is named for its characteristic helix−loop−helix Ca^{2+}-binding motif (*1*−*3*). The term EF hand refers to the spatial arrangement of the binding loop and flanking helical segments, which can be mimicked by the thumb and first two fingers of the right-hand. Within the binding loop, the coordinating groups (designated $+x$, $+y$, $+z$, $-y$, $-x$, and $-z$) are positioned at the vertexes of an octahedron. The $-y$ group is an invariant main-chain carbonyl; $-z$ is a nearly invariant glutamate; and $-x$ is frequently water. The remaining ligands are side-chain oxygen atoms—carboxylate, carbonyl, or hydroxyl. EF-hand motifs generally occur in pairs, forming an EF-hand domain. The paired motifs within a domain are joined by a short segment of antiparallel β structure.

Despite the general similarity of their metal ion-binding motifs, individual EF-hand proteins show large variations in divalent ion-binding properties. Measured Ca^{2+} dissociation constants span 4 orders of magnitude (*4*). There is substantial interest in elucidating the structural basis for these variations in metal ion affinity.

We are exploring the structure−affinity issue with select representatives of the parvalbumin (PV)[1] family (*1*−*3*, *5*). These small, vertebrate-specific proteins occupy a prominent niche in EF-hand protein lore—the first members of the superfamily extracted, purified, sequenced, and crystallized. In fact, the X-ray crystallographic structure of carp parvalbumin (*6*) established the EF-hand paradigm. Parvalbumins are believed to function as cytosolic Ca^{2+} buffers, modulating the amplitude and duration of Ca^{2+} oscillations.

The PV family includes α- and β sublineages, distinguished by isoelectric point (pI < 5 for β), C-terminal helix length (with few exceptions, one residue longer in α), and several lineage-specific sequence identities (*7*, *8*). Mammals express one α and one β isoform—which, despite 49% sequence identity, exhibit very different divalent ion-binding properties (*9*−*12*). In 0.15 M NaCl, 0.025 M Hepes, pH 7.4, the standard free energy change for Ca^{2+} binding by rat α is 3.5 kcal/mol more favorable than for rat β. There is evidence that structural features outside the EF-hand motifs influence divalent ion affinity in these two proteins (*13*, *14*).

In vivo, parvalbumins exist predominantly in their Ca^{2+}- or Mg^{2+}-bound forms. The free energy change for divalent

† This work was supported by NSF Award MCB-0131166 (to M.T.H.).

* Corresponding author. Tel.: (573) 882-7485. Fax: (573) 884-4812. E-mail: henzlm@missouri.edu.

[1] Abbreviations: ATH, avian thymic hormone, an avian β-parvalbumin; CPV3, parvalbumin isoform 3 (PV3) from chicken; CD site, parvalbumin metal ion-binding site flanked by the C and D helical segments; DSC, differential scanning calorimetry; EDTA, ethylenediaminetetraacetic acid; EF site, parvalbumin metal ion-binding site flanked by the E and F helical segments; GABA, γ-aminobutyric acid; Hepes, 4-(2-hydroxyethyl)-1-piperazineethanesulfonic acid; ITC, isothermal titration calorimetry; NMR, nuclear magnetic resonance; NTA, nitrilotriacetic acid; PV, parvalbumin; PV3, a β-parvalbumin, the third parvalbumin isoform identified in avian species.

10.1021/bi034721x CCC: $25.00
Published on Web 08/26/2003

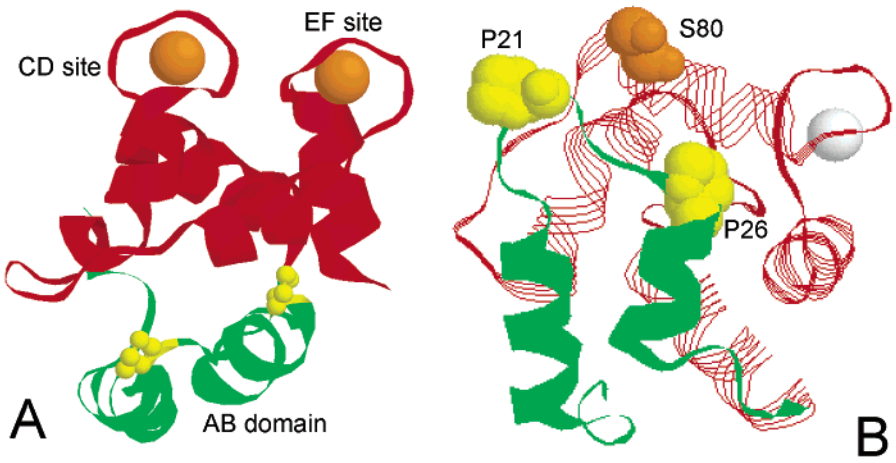

FIGURE 1: Tertiary structure of Ca^{2+}-bound rat β. (A) An overall view of the molecule emphasizing the two-domain structure. (B) A close-up of the AB domain, focusing on Pro-21 and Pro-26. Note that residues 21 and 80 appear to be well-separated in the Ca^{2+}-bound protein. These structures were created from the 1RRO PDB file (*19*).

```
          1                   10                  20                  30
RAT β     S I T D I L S A E D I A A A L Q E C Q D P D T F E P Q K F F Q T S G L S K M
RAT α     - M - - L - - - - - - K K - I G A F T A A - S - D H K - - - - M V - - K - K
CPV3      - L - - - - - - P S - - - - - - - R D - - A - - S - S - K - - - - I - - M - - K
ATH       A - - - - - - - - K - - E S - - S S - - A A - S - N Y K S - - S - V - - - S K

            40                  50                  60                  70
RAT β     S A S Q V K D I F R F I D N D Q S G Y L D G D E L K Y F L Q K F Q S D A R E
RAT α     - G D D - - K V - H I L - K - K - - F I E E - - - G S I - K G - S - - - - D
CPV3      - S - - L - E - - - I L - - - - - - - F I E E - - - - - - - - - R - E C G - - V
ATH       T P D - I - K V - G I L - Q - K - - F I E E E - - Q L - - K N - S - S - - V

                80                  90                  100
RAT β     L T E S E T K S L M D A A D N D G D G K I G A D E F Q E M V H S
RAT α     - S A K - - - T - - A - G - K - - - - - - - V E - - S T L - A E S
CPV3      - - A - - - - T F L A - - - H - - - - - - - - E - - - - - - - Q -
ATH       - - S A - - - A F L A - G - T - - - - - - - V E - - - S L - K A
```

FIGURE 2: Primary structures of rat α (*20*), rat β (*21*), chicken PV3 (*22*), and ATH (*23*, *24*).

ion binding, however, corresponds to the difference in stability between the unligated and the bound forms. Thus, the stability of the apo-form is highly relevant to discussions of binding affinity. According to conventional wisdom, α-parvalbumins should display greater intrinsic conformational stability than their β counterparts. Being more acidic, the latter have a greater net charge and should experience greater internal electrostatic repulsion. Additionally, the one-residue truncation of the F helix in the β isoform eliminates several favorable noncovalent interactions between the C-terminal carboxylate and residues 27, 31, and 36 in the B/C region of the molecule (*15*, *16*). Interestingly, however, Ca^{2+}-free rat β is significantly more stable than rat α. Whereas α denatures at 46 °C under pseudo-physiological solution conditions, β denatures at 54 °C (*17*). In 0.15 M K^+, the difference in conformational stability approaches 3.1 kcal/mol at 298 K (*18*).

Although the stabilities of Ca^{2+}-free α and β are sensitive to monovalent cation identity and concentration, the superior stability of rat β does not disappear at zero ionic strength (*18*)—indicating that it is not solely a result of enhanced interaction with solvent cations. Seeking alternative explanations for the atypical stability, our attention was drawn to the two proline residues in β—Pro-21 and Pro-26. As shown in Figure 1, Pro-21 occurs in an extended loop joining the A and B helices, and Pro-26 is the N-terminal residue of helix B. The occurrence of proline at these two positions is apparently confined to the mammalian β isoform and to one of the avian β-PV isoforms (Figure 2)—the isoform known as PV3.

Interestingly, Ca^{2+}-free PV3 from chicken (CPV3) also exhibits heightened conformational stability (vide infra), further evidence that these two residues are important structural determinants. To test this hypothesis, we have examined the consequences of replacing Pro-21 and Pro-26 in rat β with alanine, and conversely, of introducing proline at positions 21 and 26 in rat α.

MATERIALS AND METHODS

Protein Expression and Purification. Isolation schemes for ATH, CPV3, and the rat α- and β-parvalbumins have been described previously (*11*, *17*, *24*, *25*). Because the side chain of Cys-72 is solvent accessible, CPV3 undergoes facile disulfide-mediated oligomerization (*26*). To circumvent experimental complications associated with this behavior, the C72S variant of CPV3 was employed for DSC analysis.

These proteins are devoid of tryptophan, making the A_{292} value a useful criterion of homogeneity. Assuming an average

mass absorptivity at 292 nm of 0.5 $(mg/mL)^{-1}$ cm^{-1} for the contaminants, the purity of all preparations used in these studies exceeded 98%. Protein concentrations were estimated spectrophotometrically, employing $\epsilon_{274} = 3260$ M^{-1} cm^{-1} for rat β, $\epsilon_{258} = 1600$ M^{-1} cm^{-1} for rat α, and $\epsilon_{274} = 1500$ M^{-1} cm^{-1} for both CPV3 and ATH.

Site-directed mutagenesis was performed with the Quik-Change kit (Stratagene). The primers (45-mers) employed for mutagenesis were purchased from Integrated DNA Technology and used without further purification. Mutations were confirmed by automated DNA sequencing, performed at the University of Missouri DNA core facility.

Construction of an α AB/β CD-EF Chimeric Protein. Coding sequences for rat α (*20*) and β (*21*) in pET11a—cloned between the Nde I and the BamH I sites—served as the starting materials for preparation of an αAB/βCD-EF chimera. The codons for Lys-37 and Met-38 in rat β were replaced by CAATTG, the recognition sequence for Mfe I, using the Stratagene Quik-Change kit. Lys-37 and Ser-38 in rat α were similarly mutated. Codons 1−38 were then excised from the modified α sequence with Nde I and Mfe I and ligated into the modified β vector, which had been similarly digested. After confirming the sequence of this intermediate construction, residues 37 and 38 were restored to Lys and Ser, respectively, using the Quik-Change methodology, and resequenced.

Isothermal Titration Calorimetry. Prior to analysis, residual divalent metal ions were removed from protein preparations and buffers by passage over EDTA-derivatized agarose (*27*) at 4 °C. The residual Ca^{2+} content, measured by flame atomic absorption spectrometry, was less than 0.02 equiv.

Samples of Ca^{2+}-free β P21A/P26A were titrated with Ca^{2+} in a VP-ITC calorimeter (MicroCal), either alone or in the presence of a competitive chelator. Global nonlinear least-squares analysis of the data was performed with software written in-house, using a two-site Scatchard model. In the absence of a competitor, the cumulative heat of binding at the *j*th point (Q_j) in the titration is given by the expression

$$Q_j = V_o[M]_t\left[\frac{\Delta H_1 k_1[Ca^{2+}]}{1 + k_1[Ca^{2+}]} + \frac{\Delta H_2 k_2[Ca^{2+}]}{1 + k_2[Ca^{2+}]}\right] \quad (1)$$

where V_o is the sample cell volume, $[M]_t$ is the total protein concentration, k_1 and k_2 are the first and second microscopic Ca^{2+}-binding constants, and ΔH_1 and ΔH_2 are the corresponding binding enthalpies. The free Ca^{2+} concentration is estimated by solving the following mass conservation equation:

$$FX = [Ca^{2+}] + [M]_t\left[\frac{k_1[Ca^{2+}]}{1 + k_1[Ca^{2+}]} + \frac{k_2[Ca^{2+}]}{1 + k_2[Ca^{2+}]}\right] - [Ca^{2+}]_t \quad (2)$$

using $[Ca^{2+}]_t$, the known total Ca^{2+} concentration, and the current estimates of the binding constants. Note that *FX* represents the difference between the true and calculated total Ca^{2+} values. A standard bisection routine (e.g., ref *28*) is used to identify a value of $[Ca^{2+}]$ that reduces *FX* below some arbitrary threshold (e.g., $10^{-8}[Ca^{2+}]_t$).

In the presence of a competitive chelator, eqs 1 and 2 are replaced by

$$Q_j = V_o[I]_t\left[\frac{\Delta H_I K_I[Ca^{2+}]}{1 + K_I[Ca^{2+}]}\right] + V_o[M]_t\left[\frac{\Delta H_1 k_1[Ca^{2+}]}{1 + k_1[Ca^{2+}]} + \frac{\Delta H_2 k_2[Ca^{2+}]}{1 + k_2[Ca^{2+}]}\right] \quad (3)$$

$$FX = [Ca^{2+}] + [I]_t\left[\frac{K_I[Ca^{2+}]}{1 + K_I[Ca^{2+}]}\right] + [M]_t\left[\frac{k_1[Ca^{2+}]}{1 + k_1[Ca^{2+}]} + \frac{k_2[Ca^{2+}]}{1 + k_2[Ca^{2+}]}\right] - [Ca^{2+}]_t \quad (4)$$

where $[I]_t$ is the total chelator concentration, K_I is the inhibitor Ca^{2+}-binding constant, and ΔH_I is the inhibitor binding enthalpy.

Because the error associated with a bad data point has a smaller impact on the analysis, it is preferable to use the heat absorbed per injection for fitting, rather than the cumulative heat. The heat-per-injection values are calculated as the difference of successive cumulative heat terms

$$q_j = Q_j - Q_{j-1} + \left(\frac{dV}{V_o}\right)\frac{Q_j + Q_{j-1}}{2} \quad (5)$$

Q_j and Q_{j-1} are the cumulative heats of binding after the *j*th and $(j - 1)$th additions, respectively; d*V* is the volume of titrant added; and V_o is the total sample volume. The third term on the right-hand side of eq 5 corrects for the solution displaced from the cell during the *j*th addition. The actual least-squares fitting routine is based on the CURFIT algorithm from Bevington (*29*).

Parameter uncertainties were investigated by Monte Carlo analysis. *F* statistics (*30*) were used to estimate the reduced χ^2 value corresponding to the 68% confidence limit. The optimal parameter values were subjected to Gaussian smearing to generate a perturbed set of parameter values for which χ^2 was calculated. This set of parameter values was then subjected to a further round of smearing. If the χ^2 value for a given parameter set fell below the 68% limit, the values were written to a file. This process was continued until 2000 parameter sets had been collected. The reported uncertainty for each parameter represents the standard deviation for those 2000 values.

Differential Scanning Calorimetry was performed in a modified Nano DSC calorimeter (Calorimetry Sciences Corporation), equipped with cylindrical sample cells (0.32 mL active volume). The instrument response time is 5 s. Prior to analysis, samples were dialyzed to equilibrium against 0.20 M NaCl, 10 mM sodium phosphate, 5 mM EDTA, pH 7.4, and an aliquot of the dialysis reservoir served as the reference buffer. A scan rate of 1.0 deg/min was employed for all experiments. To confirm that the thermal denaturation events were thermodynamically reversible under the chosen experimental conditions, samples of the proteins were heated, cooled, and then reheated. In all cases, an endotherm was observed on the rescan, the area of which approached that of the original.

Table 1: Thermodynamic Data

protein	T_m (°C)	ΔT_m (°C)	ΔH_d (kcal/mol)	$\Delta\Delta G_{conf}$[a] (kcal/mol)	$\Delta\Delta H_{conf}$[b] (kcal/mol)	$-T\Delta\Delta S_{conf}$[c] (kcal/mol)
rat β-PV	53.6 (0.1)		76 (3)			
rat β P21A	50.4 (0.2)	−3.2[d]	72 (3)	−0.74 (0.04)	4.5	−5.2
rat β P26A	50.4 (0.2)	−3.2[d]	71 (3)	−0.74 (0.04)	4.5	−5.2
rat β P21A/P26A	46.0 (0.2)	−7.6[d]	62 (3)	−1.77 (0.04)	10.6	−12.4
CPV3 C72S	56.7 (0.2)	3.1[d]	81 (3)	0.72 (0.04)[b]	−4.3	5.1
ATH	51.9 (0.1)		73 (5)			
rat α-PV	45.8 (0.2)		72 (3)			
rat α H26P	51.4 (0.2)	5.6[e]	80 (3)	+1.25 (0.04)	−7.8	9.1
rat α A21P	37.3 (0.3)	−8.5[e]	52 (3)	−1.92 (0.06)	nd[g]	nd[g]
rat α A21P/H26P	43.6 (0.2)	−2.2[e]	62 (3)	−0.50 (0.06)	nd[g]	nd[g]
rat α/β chimera	44.2 (0.2)		52 (3)			
rat α/β A21P	50.0 (0.2)	5.8[f]	63 (3)	0.95	−8.1	8.6
rat α A21P/K80S	47.8 (0.2)	2.0[e]	75 (3)	0.45	−2.8	3.2
rat α K80S	44.5 (0.2)	−1.3[e]	71 (3)	−0.29	+1.8	−2.1

[a] Estimated with eq 7, employing the observed ΔT_m and the T_m and ΔH_d values for the wild-type protein. [b] $\Delta\Delta H_{conf}$ represents the enthalpic contribution to $\Delta\Delta G_{conf}$. It equals the change in denaturational enthalpy that occurs in going from the T_m of the variant to the wild-type T_m—i.e., $\Delta\Delta H_{conf} = -\Delta T_m \Delta C_p$, where ΔC_p is the wild-type denaturational heat capacity increment. [c] The entropic contribution to $\Delta\Delta G_{conf}$, equal to $\Delta\Delta G_{conf} - \Delta\Delta H_{conf}$. [d] Relative to wild-type rat β. [e] Relative to wild-type rat α. [f] Relative to the α/β chimera. [g] Not determined.

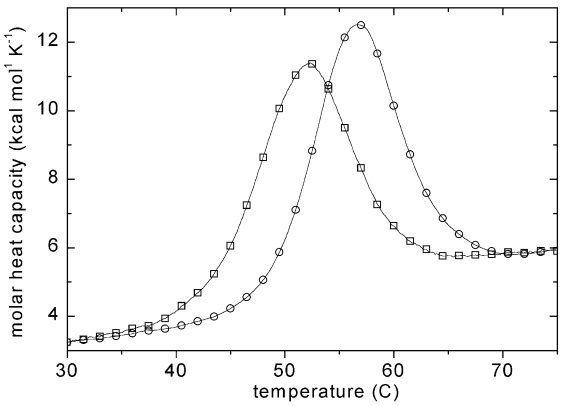

FIGURE 3: DSC analyses of Ca^{2+}-free CPV3 C72S and ATH. Representative thermal denaturation profiles are displayed for 1.0 mg/mL ATH (□) and 4.6 mg/mL chicken CPV3 C72S (○).

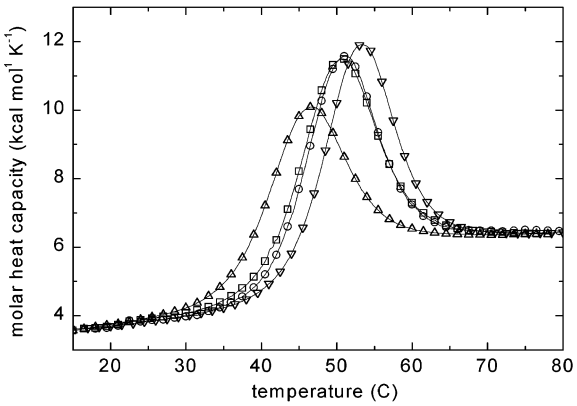

FIGURE 4: Thermal stabilities of Ca^{2+}-free rat β and the β P21A, P26A, and P21A/P26A variants. Representative DSC analyses on 5.0 mg/mL rat β (▽), 2.4 mg/mL β P21A (○), 4.2 mg/mL β P26A (□), and 8.1 mg/mL β P21A/P26A (△).

Data analysis was performed with CpCalc v. 2.1 (Applied Thermodynamics), and the reported uncertainties in T_m and ΔH_d reflect the standard deviations for at least three determinations.

RESULTS

CPV3 and ATH Exhibit Enhanced Conformational Stability. Avian species express two β isoforms, both of which were discovered in thymus tissue. Named for its capacity to stimulate avian T-cell maturation and proliferation (*31*−*33*), avian thymic hormone (ATH, pI 4.3) was detected and purified to homogeneity by Ragland and coworkers (*34*, *35*). This laboratory subsequently identified a second β isoform in avian thymic extracts (*24*), which was christened PV3. The sequence of chicken PV3 (CPV3, pI 4.6) is noteworthy for its 69% identity with the rat β sequence and attenuated divalent cation affinity.

Like rat β, the CPV3 primary structure harbors proline residues at positions 21 and 26. Significantly, Ca^{2+}-free CPV3 also exhibits atypical thermal stability (Figure 3, ○; Table 1), consistent with the notion that Pro-21 and Pro-26 contribute to the anomalous stability of rat β. At 56.7 °C, the melting temperature of PV3 is fully 3.1° higher than rat β—possibly due to the presence of a third proline residue at position 8 (vide infra).

The relative thermal stability of ATH is also shown in Figure 3 (□). Although Pro-21 and Pro-26 are absent in this isoform, the ATH sequence does include a proline residue, at position 40. Consistent with the potential stabilizing influence of this residue, discussed later, the melting point of ATH (51.9 °C) is higher than that of rat α under our standard analysis conditions but lower than those of rat β and CPV3. For comparison, carp parvalbumin (pI 4.25), a β isoform lacking proline residues, exhibits thermal stability comparable to rat α (*36*).

Site-Specific Replacement of Pro-21 and Pro-26 in Rat β. The impact of replacing Pro-21 and Pro-26 by alanine is displayed in Figure 4. As suggested by the near superposition of their DSC scans, P21A (○) and P26A (□) have nearly identical effects on stability, each decreasing T_m by 3.2°. Simultaneous replacement of the two residues produces a ΔT_m of −7.6°, perceptibly larger than the sum of the individual T_m shifts. The thermal stability of the β P21A/P26A double variant approaches that of wild-type rat α—suggesting that Pro-21 and Pro-26 are primary determinants of the exceptional stability of rat β.

The denaturational heat capacity increments for rat α and β are both 1.4 kcal mol^{-1} K^{-1} (*18*). The changes in denaturational enthalpy observed for the β P21A and P26A

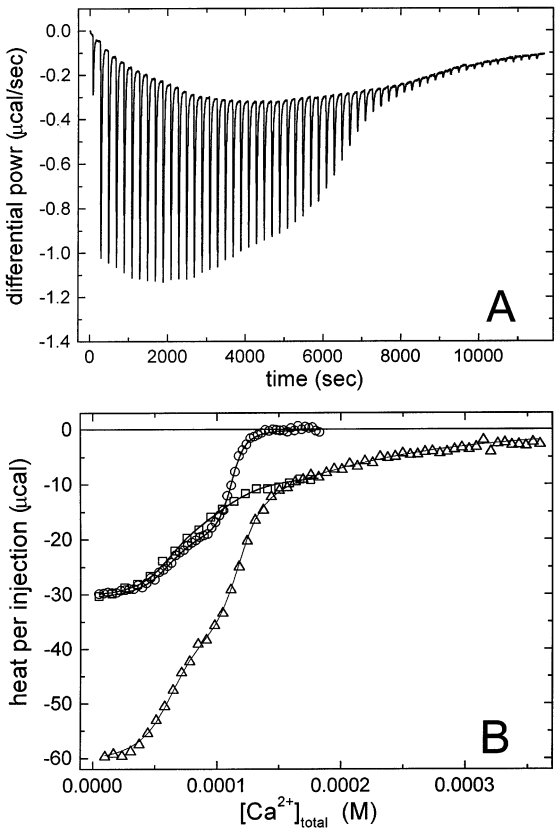

FIGURE 5: Measurement of β P21A/P26A Ca^{2+} affinity by competitive isothermal titration calorimetry. (A) Raw data for the titration of 62 μM β P21A/P26A with 1.0 mM Ca^{2+}, at pH 7.4, in 0.15 M NaCl, 0.025 M Hepes, pH 7.4. (B) Integrated ITC data. Titration of 62 μM β P21A/P26A with 1.0 mM Ca^{2+} (○); titration of 62 μM β P21A/P26A with 2.0 mM Ca^{2+} in the presence of 0.125 mM NTA (△); and titration of 62 μM β P21A/P26A with 1.0 mM Ca^{2+} in the presence of 10 mM NTA (□). The solid lines represent the best least-squares fit to the composite data set. The reduced χ^2 value for the weighted fit is 1.66.

variants are consistent with a ΔC_p value of this magnitude, suggesting that these mutations cause minor structural perturbations.

To determine whether simultaneous replacement of Pro-21 and Pro-26 provokes substantial alterations in divalent ion-binding behavior, the Ca^{2+} affinity of β P21A/P26A was measured by ITC. Representative raw data for the titration of P21A/P26A with Ca^{2+} are shown in Figure 5A. Corresponding integrated data are shown in 5B (○); additionally, samples of the protein were also titrated in the presence of a competitive chelator, nitrilotriacetic acid (NTA) (△, □). The presence of the competitor increases the curvature in the binding isotherms, permitting a more accurate determination of the binding constant.

Under the chosen solution conditions, NTA binds a single equivalent of Ca^{2+} with an association constant of 1.17×10^4 M^{-1} and an apparent binding enthalpy of -1960 cal/mol. The integrated data from the titrations conducted in the absence and presence of the chelator were subjected to global nonlinear least-squares analysis, as described in the Materials and Methods. The optimal fit, indicated by the solid lines in Figure 5B, yields estimates for K_1 and K_2 of 2.60 (0.17) $\times 10^7$ M^{-1} and 1.32 (0.04) $\times 10^6$ M^{-1}. Uncertainties were estimated by Monte Carlo analysis. Figure 6 displays 2000 randomly generated parameter sets meeting the requisite χ^2 criterion, plotted as a function of χ^2.

The corresponding binding constants determined for wild-type β by a somewhat more extensive ITC analysis (*37*) were 2.39 (0.10) $\times 10^7$ M^{-1} and 1.52 (0.05) $\times 10^6$ M^{-1}. Previous flow-dialysis measurements on rat β have yielded estimates of 2.30 (0.1) $\times 10^7$ M^{-1} for k_1 and 1.10 (0.15) $\times 10^6$ M^{-1} for k_2 (*11, 13*).

Site-Specific Replacement by Ala-21 and His-26 by Pro in Rat α. Having demonstrated that the presence of proline at positions 21 and 26 substantially increases conformational stability in rat β, it was of interest to examine the generality of the effect. Toward this end, proline residues were introduced at positions 21 and 26 in rat α.

DSC data for the resulting variants are presented in Figure 7. Pro-26 significantly stabilizes rat α, raising the T_m by 5.6°. Pro-21 (□), by contrast, has a pronounced destabilizing effect, lowering the T_m by 8.5°. As observed for the β P21A/P26A variant, the effects of the A21P and H26P mutations are not exactly additive. Whereas the temperature shifts for the individual mutations sum to −2.9°, the α A21P/H26P (○) variant displays a melting temperature just 2.2° lower than wild-type α (△).

Stability of an α *AB/*β *CD-EF Chimera. Impact of the A21P Mutation.* The destabilization of the α isoform produced by the A21P mutation was believed to result from a steric conflict with a nearby side chain. To test this hypothesis, we produced a chimeric protein (α/β)—in which the α AB domain is fused to the β CD-EF domain—then mutated Ala-21 to proline (α/β A21P).

The DSC thermograms for α/β (□) and α/β A21P (○) are displayed in Figure 8. Although the T_m for the chimeric protein (44.2°) is comparable to wild-type α, the ΔH_d for α/β (52 ± 3 kcal/mol) is significantly lower than that of wild-type α (72 ± 3 kcal/mol)—presumably an indication of suboptimal complementarity between the α-AB and the β-CD/EF surfaces. Importantly, however, the A21P mutation has a very different impact in the chimera. Whereas A21P lowered the T_m for wild-type α from 45.8 to 37.3°, the mutation raises the T_m of α/β from 44.2 to 50.0 °C. This finding supports the idea of a steric conflict in α A21P between Pro-21 and one or more residues in the α CD/EF domain.

Stability of α *K80S and* α *A21P/K80S.* In Ca^{2+}-bound rat β, Pro-21 is adjacent to Arg-75 and Thr-78. Inspection of the rat α and β sequences in this vicinity reveals just one position at which the α isoform has the bulkier side chain. Whereas residue 80 is serine in β, it is lysine in α. Accordingly, we introduced the K80S mutation into α A21P. The DSC data for the α K80S (□) and α A21P/K80S (○) variants are displayed in Figure 9. For comparison, the behavior of wt α (dotted line) and α A21P (dashed line) are also presented. Significantly, when Lys-80 is replaced by serine, Pro-21 assumes a stabilizing role. α K80S is slightly less stable than wt α (T_m = 44.5 °C). The A21P mutation raises the T_m of α K80S to 47.8 °C— fully 2.0° higher than wild-type α.

DISCUSSION

Proline occurs with roughly average frequency, accounting for 5.1% of the residues in a survey of 1021 unrelated

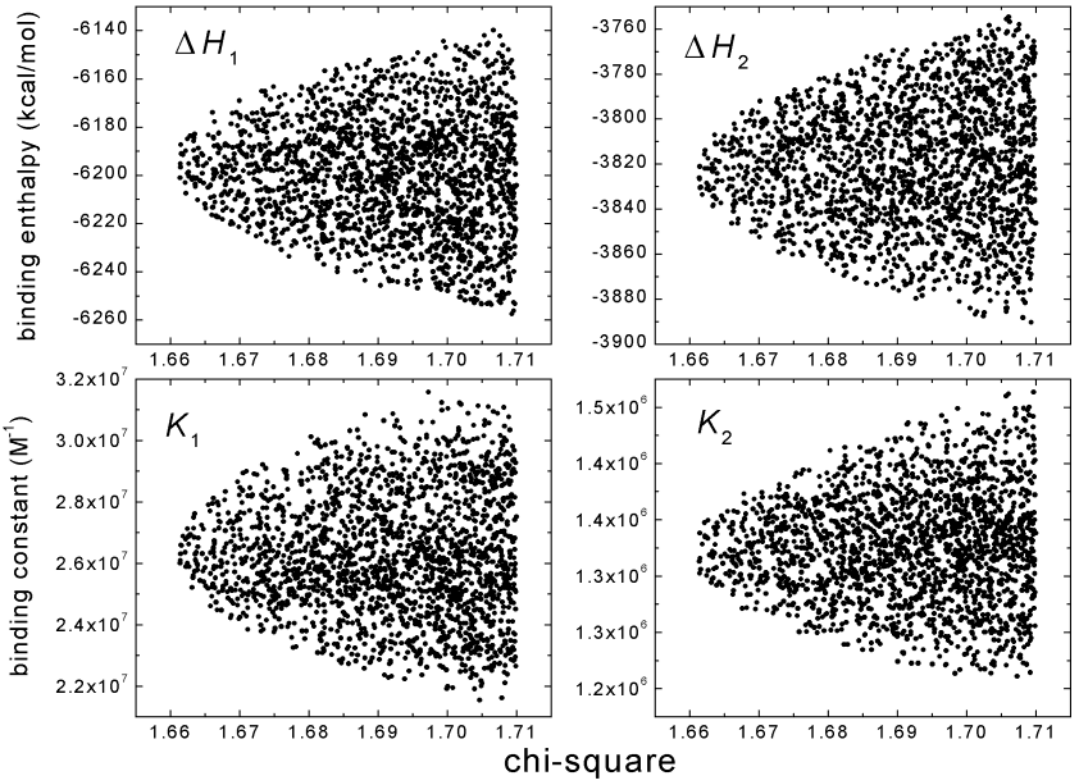

FIGURE 6: Evaluation of β P21A/P26A Ca^{2+}-binding parameter uncertainties. The optimal binding parameters determined by least-squares minimization were subjected to repeated Gaussian smearing, and χ^2 values were determined for the resulting parameter sets. 2000 parameter sets yielding χ^2 values within the 68% confidence interval determined by F statistics (1.66−1.71) were retained and have been plotted in this figure vs χ^2.

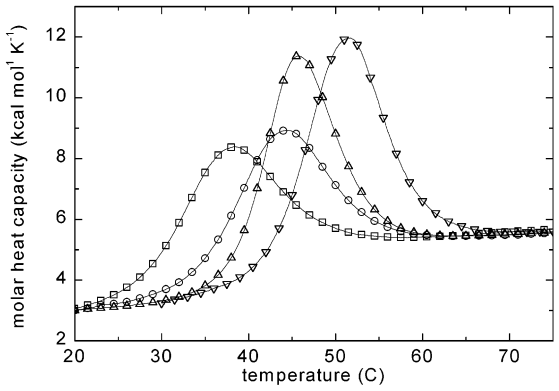

FIGURE 7: Impact of the α A21P, H26P, and A21P/H26P mutations on the thermal stability of Ca^{2+}-free rat α. DSC thermograms are displayed for 3.4 mg/mL wild-type rat α (△), 6.6 mg/mL α A21P (□), 2.8 mg/mL α H26P (▽), and 5.8 mg/mL α A21P/H26P (○).

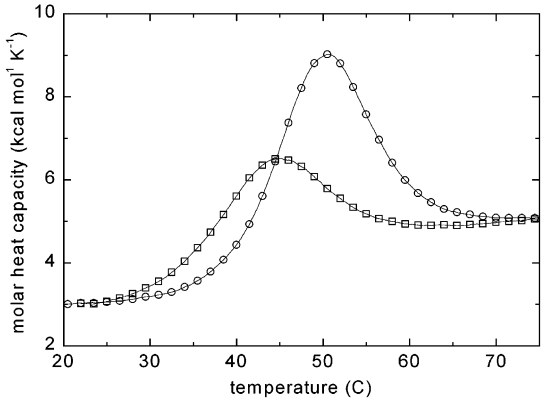

FIGURE 8: Thermal stabilities of the Ca^{2+}-free α/β chimera and the α/β A21P variant. The chimeric protein produced from the α AB domain and the β CD-EF domain (□) was studied by scanning calorimetry at a concentration of 3.1 mg/mL. The A21P site-specific variant of α/β (○) was examined at a concentration of 6.5 mg/mL.

proteins (*38*). Its presence has two major energetic consequences. The C_3 alicyclic side chain—bridging C_α and the amino group—fixes the proline ϕ angle at approximately −60° and also restricts the ϕ and ψ angles of the preceding residue. Second, although the trans form of ω—the torsional angle about the peptide bond—is otherwise favored by a factor of 10^3 (*39*), the energetic preference is much lower if the succeeding residue is proline. In unstructured proteins and short linear peptides, the cis proline content ranges from 5 to 30% (*40*, *41*); in folded proteins, it is on the order of 7% (*42*).

The work described herein is relevant to the first of these two issues. Residues 21 and 26 in parvalbumin both exist in secondary structural elements compatible with proline. The backbone changes direction at residue 21, and proline commonly occurs as the second residue in type I and II β bends (reverse turns). Residue 26 marks the start of the parvalbumin B helix. Although rare in the central regions of α helices, because of its inability to serve as hydrogen bond donor, proline is not uncommon at the N-terminus. The peptide bonds that precede Pro-21 and Pro-26 in rat β both adopt the trans configuration in the Ca^{2+}-bound protein (*19*).

Although the impact of a specific residue on conformational free energy can have both enthalpic and entropic contributions, the changes in stability described herein are largely attributable to conformational entropy effects. Because proline itself has limited conformational options and

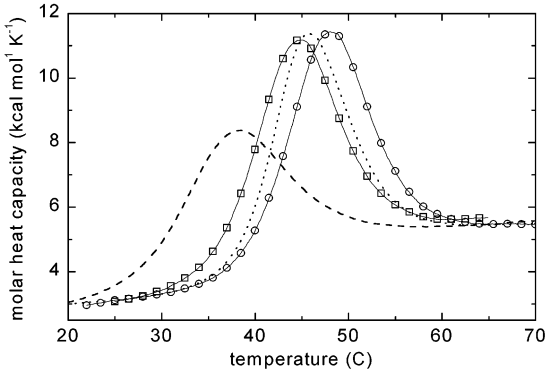

FIGURE 9: K80S mutation abolishes steric clash in α A21P. DSC thermograms for 5.3 mg/mL α K80S (□) and 4.6 mg/mL α A21P/K80S (○). Traces for wild-type α (dotted) and α A21P (dashed) are also included for comparison.

restricts the conformation of the preceding residue, it should confer entropic stability at locations compatible with its presence (*43*). Matthews et al. (*44*) examined the stability of the A82P mutation in the T4 lysozyme. Position 82 was selected on the basis of proline conformational requirements and minimal opportunities for steric interference or noncovalent side-chain interactions. Their analysis yielded a $\Delta\Delta G_{conf}$ value of +0.8 kcal/mol for the mutation, where ΔG_{conf} symbolizes the free energy change for the unfolding reaction. In other words, the replacement of Ala-82 by proline stabilized the folded form of T4 lysozyme by 0.8 kcal/mol. Because the structure of the A82P variant was identical to wild-type T4 lysozyme, excepting the presence of the Pro-82 side chain, the authors concluded that the increased stability was solely attributable to entropic effects.

Assuming that the entropy of unfolding for residue *Y* is related to the area of a Ramachandran plot accessible to that residue (γ_Y), then the change in main-chain conformational entropy ($\Delta\Delta S_{conf}$) that accompanies substitution of residue Y by residue Z should equal

$$\Delta\Delta S_{conf} = R \ln(\gamma_Z/\gamma_Y) \quad (6)$$

where *R* is the gas constant (*45*). This treatment predicts that replacement of alanine by proline in an unfolded polypeptide should produce a $T\Delta\Delta S_{conf}$ value of −1.4 kcal/mol at 338 K, the T_m for wild-type T4 lysozyme. Accordingly, the folded peptide should be stabilized by this amount. This theoretical value is 0.6 kcal/mol greater than that measured for the A82P T4 lysozyme variant.

The 0.6 kcal/mol discrepancy between the predicted and the observed values—i.e., 1.4 versus 0.8 kcal/mol—was attributed by Matthews et al. (*44*) to deficiencies in the theory. In fact, subsequent free energy simulations by Yun et al. (*46*) suggested that eq 6 may overestimate $\Delta\Delta S_{conf}$. For example, the latter investigators determined that substitution of proline for alanine at the N-terminus of a helix should produce a $\Delta\Delta G_{conf}$ value of 1.1 kcal/mol at 338 K. This correction would reduce the discrepancy between calculated and observed $\Delta\Delta G_{conf}$ values for A82P from 0.6 to 0.3 kcal/mol. Although there are currently no precise estimates of proline side-chain entropy, the residual 0.3 kcal/mol difference might plausibly reflect the increase in side-chain conformational entropy resulting from the replacement of alanine by proline. In other words, whereas the mutation would reduce backbone conformational entropy by 1.1 kcal/mol, side-chain entropy would increase by 0.3 kcal/mol, producing the observed 0.8 kcal/mol net stabilization. Alternatively, the 0.3 kcal/mol discrepancy might reflect a solvation penalty for the bulkier proline side chain.

Energetics of the P21A and P26A Mutations in Rat β. In the present study, replacement of either Pro-21 or Pro-26 by alanine in rat β-parvalbumin lowers the T_m by 3.2 °C. The denaturational enthalpies measured for β P21A and β P26A suggest that the mutations have a minimal impact on the ΔC_p for denaturation. Accordingly, the following relationship derived by Becktel and Schellman (*47*) can be used to estimate the change in conformational free energy:

$$\Delta\Delta G^{\circ\prime} = \frac{\Delta T_m(\Delta H_d)}{T_m} \quad (7)$$

Assuming $\Delta T_m = -3.2°$ and employing the ΔH_d and T_m values for wild-type rat β (76 kcal/mol and 326.85 K, respectively), eq 7 yields a $\Delta\Delta G$ value of −0.74 kcal/mol for either mutation. The magnitude of the alteration agrees well with that reported by Matthews et al. for the T4 lysozyme A82P mutation.

Assuming that the ΔC_p for denaturation is unchanged in the variant proteins, the entropic nature of the destabilization resulting from the P21A and P26A mutations can be readily demonstrated. It is evident that the $\Delta\Delta G_{conf}$ estimate for a particular mutation must correspond to the ΔG_{conf} of the variant protein at the T_m of the reference protein. In the present case, the conformational free energy change for P21A (or P26A) will equal −0.74 kcal/mol at 53.6 °C, the T_m for wild-type rat β. The enthalpic contribution to $\Delta\Delta G_{conf}$—i.e., $\Delta\Delta H_{conf}$—is obtained by multiplying ΔC_p (1.4 kcal mol^{-1} K^{-1}) by the T_m difference (53.6−50.4). The entropic contribution, $-T\Delta\Delta S_{conf}$, is then equal to $\Delta\Delta G_{conf} - \Delta\Delta H_{conf}$. For P21A and P26A, the $\Delta\Delta H_{conf}$ and $-T\Delta\Delta S_{conf}$ values are 4.5 and −5.2 kcal/mol, respectively. Thus, the reduction in stability results from a more favorable entropy change upon denaturation—consistent with replacement of proline by a residue having higher backbone conformational entropy. Similar analyses have been performed on a subset of the other variant proteins examined in this study, and the results have been included in Table 1.

The ΔT_m determined for the P21A/P26A double variant exceeds the sum of T_m shifts for the individual mutations by 1.2°. This effect could conceivably indicate a cooperative interaction between the two residues. Alternatively, it might reflect a small decrease in the ΔC_p value for the protein. Consistent with the latter hypothesis, the ΔH_d value determined for β P21A/P26A (62 kcal/mol) is slightly smaller than expected. For a ΔT_m of 7.6°, the predicted ΔH_d value for β P21A/P26A, if ΔC_p were unchanged, would be 66 kcal/mol.

The relative thermal stabilities of chicken PV3 and rat β are also relevant to the discussion of Ala ↔ Pro substitutions. As noted earlier, the T_m for the CPV3 isoform is 3.1° higher than that of rat β. Assuming that the ΔC_p for denaturation of CPV3 is comparable to that of rat β—a reasonable assumption, considering their 69% sequence identity—eq 7 yields a $\Delta\Delta G_{conf}$ value of 0.72. It is tempting to ascribe the increased stability of CPV3—similar in magnitude to the stability reduction caused by the β P21A and β P26A

mutations—to the presence of proline, rather than alanine, at position 8. Indeed, dissection of the $\Delta\Delta G_{conf}$ for CPV3, relative to rat β, into its component terms (Table 1) indicates that the greater stability of the avian isoform derives from a less favorable entropy of unfolding—i.e., $-T\Delta\Delta S_{conf}$ is positive and exceeds $\Delta\Delta H_{conf}$ in magnitude.

Energetics of the α H26P Mutation. Rat β is destabilized to a similar extent if either Pro-21 or Pro-26 is replaced by alanine. By contrast, the consequences of introducing proline at these locations in rat α are position-dependent. Whereas Pro-26 substantially raises the melting temperature, Pro-21 sharply lowers it. The H26P substitution is discussed first.

Estimates for the configurational entropy of the histidine side chain, relative to alanine, range from 0.95 (*48*) to 1.27 kcal/mol (*49*−*51*). In the absence of other energetic contributions, the $\Delta\Delta G_{conf}$ value for an H → P substitution should be between 1.7 and 2.0 kcal/mol—i.e., 0.95−1.27 kcal/mol greater than the corresponding value for an A → P substitution. In fact, replacement of His-26 by proline in rat α produces a T_m shift of 5.6°. Substituting this value into eq 7, along with the T_m and H_d values for rat α (318.95 K and 72 kcal/mol, respectively) yields a $\Delta\Delta G_{conf}$ of 1.25 kcal/mol for H26P. This value is 0.45−0.75 kcal/mol lower than anticipated, suggesting that the H26P mutation is accompanied by an unfavorable enthalpic contribution. Possibilities would include steric interference, solvation penalty, loss of stabilizing van der Waals interactions, or loss of a hydrogen bond. This enthalpic effect notwithstanding, the $-T\Delta\Delta S_{conf}$ term obtained from a dissection of $\Delta\Delta G_{conf}$ is positive—i.e, the denaturational entropy change is less favorable—consistent with the replacement of histidine by a residue (proline) having a lower conformational entropy.

Energetics of the α A21P Mutation. Rather than stabilizing the protein, A21P significantly lowers the T_m. The mutation also produces a large decrease in ΔH_d, suggesting that it does not qualify as a minimal perturbation of the α isoform. Accordingly, the accuracy of the $\Delta\Delta G_{conf}$ value calculated with eq 7 (−1.92 kcal/mol) is suspect, and no attempt has been made to parse the $\Delta\Delta G_{conf}$ estimate into enthalpic and entropic contributions. The unexpected decrease in stability and sharp reduction in ΔH_d implied the existence of a steric conflict between Pro-21 and an adjacent residue in the α CD-EF domain.

To test this hypothesis, we examined the impact of the A21P mutation in a chimeric protein produced by fusing the α AB domain to the β CD/EF domain. A21P stabilizes the α/β chimera by 5.8°. Substituting the T_m and ΔH_d values for wild-type α/β (317.35 K and 52 kcal/mol) into eq 7 yields an estimate for $\Delta\Delta G_{conf}$ of 0.95 kcal/mol. This result supports the contention that the presence of proline at position 21 is sterically incompatible with the Ca^{2+}-free α metal ion-binding domain. By placing the α A21P AB domain in the context of the β CD-EF domain, steric interference is eliminated, and the mutation exerts a stabilizing effect comparable in magnitude to the destabilization resulting from the reverse mutation in rat β. The $-T\Delta\Delta S_{conf}$ value associated with the A21P mutation in α/β is positive, consistent with a reduction in the denaturational entropy.

In the Ca^{2+}-bound form of β, Pro-21 contacts Arg-75 and Thr-78. Neither residue is likely, however, to be the source of the putative steric conflict. Arg-75 is invariant, and replacement of Thr-78 by serine (the residue present at position 78 in α) should not produce interference. It is more likely that Pro-21 has different nearest neighbors in the Ca^{2+}-free state.

The task of identifying the noncompatible residue in the α CD/EF domain was simplified by the similarity of α and β between residues 72 and 86 (Figure 2). The sequences are identical at 10 positions, highly conserved at three others. The two nonconservative substitutions in this region occur at positions 79 (Ala in α, Glu in β) and 80 (Lys in α, Ser in β), and only the latter places the bulkier side chain in α. Accordingly, the α K80S and α A21P/K80S variants were prepared and characterized.

The K80S mutation alone has a minor destabilizing impact ($\Delta\Delta G_{conf} = -0.29$ kcal/mol). Replacement of Ala-21 by proline in K80S produces a T_m shift of 3.3°, so that the melting temperature of α A21P/K80S (47.8 °C) is 2.0° higher than wild-type α. The corresponding $\Delta\Delta G_{conf}$ for the mutation, calculated with eq 7, is 0.74 kcal/mol. This value is identical in magnitude, although of course opposite in sign, to the $\Delta\Delta G_{conf}$ value calculated for the P21A mutation in rat β. The $-T\Delta\Delta S_{conf}$ term associated with replacement of Ala-21 with proline in K80S is 5.3 kcal/mol, indicating that the mutation produces the anticipated decrease in denaturational entropy. Please note that the $\Delta\Delta G_{conf}$ and $-T\Delta\Delta S_{conf}$ values listed in Table 1 for α K80S and α A21P/K80S have been calculated relative to wild-type α. They must be combined to obtain the corresponding parameters for the A21P mutation in α K80S.

Evidently, then, Lys-80 is responsible for the steric interference observed in α A21P. Given that residues 21 and 80 are well-separated in the Ca^{2+}-bound protein (see Figure 1B), the conformations of the apo- and Ca^{2+}-bound forms must differ substantially. This conclusion is consistent with previous NMR and optical spectroscopic data from several laboratories (e.g., refs *14* and *52*−*55*).

As observed for β 21/26, the ΔT_m measured for the α A21P/H26P double variant does not equal the sum of the temperature shifts for the individual mutations. Whereas the ΔT_m values for the A21P and H26P mutations sum to −2.9°, the T_m for α 21/26 is just 2.2° lower than for wild-type α. This discrepancy may reflect a conformational interaction between the two proline residues. In other words, replacement of His-26 by proline partially relieves the steric clash between Pro-21 and the α CD-EF domain.

Impact of Proline Mutations on Rat β Ca^{2+} Affinity. Although simultaneous replacement of Pro-21 and Pro-26 with alanine residues in rat β yields a protein with stability comparable to rat α, these two mutations alone do not significantly raise Ca^{2+} affinity. This result is somewhat unexpected. Using the isolated AB and CD-EF fragments from pike parvalbumin, Permyakov et al. (*56*) have shown that association of the AB and CD-EF domains is thermodynamically linked to the Ca^{2+}-binding events. Moreover, a recent NMR dynamics study by this lab suggests that the AB and D/E regions of rat β are more ordered in the Ca^{2+}-free state (*14*), implying that the AB domain is sensitive to the divalent ion-binding events. Conversely, an alteration of the conformational energetics of the AB domain could reasonably have been expected to perturb Ca^{2+}-binding affinity. The minimal impact of the P21A/P26A double mutation on Ca^{2+} affinity suggests that communication

between the AB and the CD-EF domains is mediated by other, presently unidentified, residues in the protein.

Concluding Remarks. The atypical conformational stabilities of rat β and chicken PV3 are apparently due to the proline residues at positions 21 and 26. Replacement of these two residues by alanine in rat β abolishes the protein's excess stability. Conversely, rat α is significantly stabilized by substitution of proline for His-26. Although replacement of Ala-21 by proline lowers the T_m of wild-type rat α, the A21P mutation stabilizes an α/β chimera, presumably due to elimination of steric interference. Except for the steric clash in α A21P—which was traced to Lys-80—the alterations in stability that accompany proline addition/removal are consistent with the predicted changes in peptide backbone and amino acid side-chain conformational entropies.

Because the physiological roles of rat β and CPV3 are presently unknown, the functional significance of Pro-21 and Pro-26, if any, remains conjectural. Interestingly, both proteins are expressed in the auditory organs of their respective species. The mammalian β isoform is present in the outer hair cells (*57*, *58*)—cells that are believed to facilitate perception of weak acoustic signals (*59*). In fact, the outer hair cell is currently believed to be the sole site of β expression in postnatal mammals.

Like ATH, chicken PV3 was discovered in thymus tissue (*24*, *60*), and a role in avian T-cell maturation or function has been suggested (*61*). Recently, however, PV3 has been detected in the sensory hair cells of avian and amphibian auditory organs (*62*). In the bullfrog, the PV3 concentration is estimated at 3 mM.

Presumably, these parvalbumin isoforms function as mobile cytosolic Ca^{2+} buffers in these settings. However, the physiological rationale for their recruitment is not obvious. In other tissues—notably fast-twitch muscle, GABAergic neurons, and even the inner hair cells of the auditory organ (*63*)—the α isoform is seemingly the default Ca^{2+} buffer. Conceivably, the mammalian β isoform and PV3 were selected because their divalent ion-binding properties are more closely tuned to peculiarities of the mammalian outer hair cell and avian/amphibian hair cell physiology.

REFERENCES

1. Kretsinger, R. H. (1980) Structure and evolution of calcium modulated proteins, *CRC Crit. Rev. Biochem. 8*, 115−164.
2. Kawasaki, H., and Kretsinger, R. H. (1994) Calcium-binding proteins 1: EF hands, *Protein Profile 1*, 343−517.
3. Celio, M. R., Pauls, T., and Schwaller, B. (1996) *Guidebook to the Calcium-Binding Proteins*, Oxford University Press, New York.
4. Seamon, K. B., and Kretsinger, R. H. (1983) Calcium-modulated proteins, in *Calcium in Biology* (Spiro, T. G., Ed.) pp 3−51, John Wiley and Sons, New York.
5. Wnuk, W., Cox, J. A., and Stein, E. A. (1982) Parvalbumins and other soluble high-affinity calcium-binding proteins from muscle, *Calcium Cell. Funct. 2*, 243−278.
6. Kretsinger, R. H., and Nockolds, C. E. (1973) Carp muscle calcium-binding protein. II. Structure determination and general description, *J. Biol. Chem. 248*, 3313−3326.
7. Goodman, M., and Pechère, J.-F. (1977) The evolution of muscular parvalbumins investigated by the maximum parsimony method, *J. Mol. Evol. 9*, 131−158.
8. Nakayama, S., Moncrief, N. D., and Kretsinger, R. H. (1992) Evolution of EF-hand calcium-modulated proteins. II. Domains of several subfamilies have diverse evolutionary histories, *J. Mol. Evol. 34*, 416−448.
9. Pauls, T. L., Durussel, I., Cox, J. A., Clark, I. D., Szabo, A. G., Gagne, S. M., Sykes, B. D., and Berchtold, M. W. (1993) Metal binding properties of recombinant rat parvalbumin wild-type and F102W mutant, *J. Biol. Chem. 268*, 20897−20903.
10. Eberhard, M., and Erne, P. (1994) Calcium and magnesium binding to rat parvalbumin, *Eur. J. Biochem. 222*, 21−26.
11. Hapak, R. C., Lammers, P. J., Palmisano, W. A., Birnbaum, E. R., and Henzl, M. T. (1989) Site-specific substitution of glutamate for aspartate at position 59 of rat oncomodulin, *J. Biol. Chem. 264*, 18751−18760.
12. Cox, J. A., Milos, M., and MacManus, J. P. (1990) Calcium- and magnesium-binding properties of oncomodulin, *J. Biol. Chem. 265*, 6633−6637.
13. Henzl, M. T., Hapak, R. C., and Likos, J. J. (1998) Interconversion of the ligand arrays in the CD and EF sites of oncomodulin. Influence on Ca^{2+}-binding affinity, *Biochemistry 37*, 9101−9111.
14. Henzl, M. T., Wycoff, W. G., Larson, J. D., and Likos, J. J. (2002) ^{15}N nuclear magnetic resonance relaxation studies on rat β-parvalbumin and the penta-carboxylate variants, S55D and G98D, *Protein Sci. 11*, 158−173.
15. Padilla, A., Cavé, A., and Parello, J. (1988) Two-dimensional ^1H nuclear magnetic resonance study of pike pI 5.0 parvalbumin (Esox lucius), *J. Mol. Biol. 204*, 995−1017.
16. McPhalen, C. A., Sielecki, A. R., Santarsiero, B. D., and James, M. N. G. (1994) Refined crystal structure of rat parvalbumin, a mammalian α-lineage parvalbumin, at 2.0 Å resolution, *J. Mol. Biol. 235*, 718−732.
17. Henzl, M. T., and Graham, J. S. (1999) Conformational stabilities of the rat α- and β-parvalbumins, *FEBS Lett. 442*, 241−245.
18. Henzl, M. T., Larson, J. D., and Agah, S. (2000) Influence of monovalent cations on rat α- and β-parvalbumin stabilities, *Biochemistry 39*, 5859−5867.
19. Ahmed, F. R., Rose, D. R., Evans, S. V., Pippy, M. E., and To, R. (1993) Refinement of recombinant oncomodulin at 1.30 Å resolution, *J. Mol. Biol. 230*, 1216−1224.
20. Epstein, P., Means, A. R., and Berchtold, M. W. (1986) Isolation of a rat parvalbumin gene and full-length cDNA, *J. Biol. Chem. 261*, 5886−5891.
21. Gillen, M. F., Banville, D., Rutledge, R. G., Narang, S., Seligy, V. L., Whitfield, J. F., and MacManus, J. P. (1987) A complete complementary DNA for the oncodevelopmental calcium-binding protein, oncomodulin, *J. Biol. Chem. 262*, 5308−5312.
22. Brewer, J. M., Wunderlich, J. K., and Ragland, W. L. (1990) The amino acid sequence of avian thymic hormone, a parvalbumin, *Biochimie 72*, 653−660.
23. Palmisano, W. A., and Henzl, M. T. (1991) Molecular cloning of the thymus-specific parvalbumin designated 'avian thymic hormone': isolation of a full-length cDNA and expression of the recombinant protein in *Escherichia coli*, *Arch. Biochem. Biophys. 285*, 211−220.
24. Hapak, R. C., Zhao, H., Boschi, J. M., and Henzl, M. T. (1993) Novel avian thymic parvalbumin exhibits high degree of sequence homology to oncomodulin, *J. Biol. Chem. 269*, 5288−5296.
25. Serda, R. E., and Henzl, M. T. (1991) Metal ion-binding properties of the thymus-specific parvalbumin known as avian thymic hormone, *J. Biol. Chem. 266*, 7291−7299.
26. Hapak, R. C., Zhao, H., and Henzl, M. T. (1994) Oligomerization of an avian thymic parvalbumin: chemical evidence for a Ca^{2+}-specific conformation, *FEBS Lett. 349*, 295−300.
27. Haner, M., Henzl, M. T., Raissouni, B., and Birnbaum, E. R. (1984) Synthesis of a new chelating gel: removal of Ca^{2+} ions from parvalbumin, *Anal. Biochem. 138*, 229−234.
28. Nyhoff, L., and Leestma, S. (1995) *Fortran 77 and Numerical Methods for Engineers and Scientists*, Prentice-Hall, Englewood Cliffs, NJ.
29. Bevington, P. R. (1969) *Data reduction and Error Analysis for the Physical Sciences*, McGraw-Hill, Boston.
30. Bevington, P. R., and Robinson, D. K. (1992) *Data Reduction and Error Analysis for the Physical Sciences, 2nd ed.*, McGraw-Hill, Boston.
31. Pace, J. L., Barger, B. O., Dawe, D. L., and Ragland, W. L. (1978) Specific antigens of chicken thymus, *Eur. J. Immunol. 8*, 671−678.
32. Murthy, K. K, and Ragland, W. L. (1984) Immunomodulation by thymic hormones: studies with an avian thymic hormone, in *Chemical Regulation of Immunity in Veterinary Medicine*, pp 481−491, A. R. Liss, New York.
33. Murthy, K. K., Beach, F. G., and Ragland, W. L. (1984) Expression of T-cell markers on chicken bone marrow precursor cells

incubated with an avian thymic hormone, in *Thymic Hormones and Lymphokines* (Goldstein, A. L., Ed.) pp 375−382, Plenum, New York.
34. Brewer, J. M., Wunderlich, J. K., Kim, D. H., Carr, M. Y., Beach, G. G., and Ragland, W. L. (1989) Avian thymic hormone (ATH) is a parvalbumin, *Biochem. Biophys. Res. Commun. 160*, 1155−1161.
35. Barger, B., Pace, J. L., and Ragland, W. L. (1991) Purification and partial characterization of an avian thymic hormone, *Thymus 17*, 181−197.
36. Filimonov, V. V., Pfeil, W., Tsalkova, T. N., and Privalov, P. L. (1978) Thermodynamic investigations of proteins IV. Calcium-binding protein parvalbumin, *Biophys. Chem. 8*, 117−122.
37. Henzl, M. T., Larson, J. D., and Agah, S. (2003) Estimation of parvalbumin Ca^{2+}- and Mg^{2+}-binding constants by global least-squares analysis of isothermal titration calorimetry data, *Anal. Biochem. 319*, 216−233.
38. McCaldon, P., and Argos, P. (1988) Oligopeptide biases in protein sequences and their use in predicting protein coding regions in nucleotide sequences, *Proteins 4*, 99−122.
39. Brandts, J. F., Halvorson, H. R., and Brennan, M. (1975) Consideration of the possibility that the slow step in protein denaturation reactions is due to cis−trans isomerization of proline residues, *Biochemistry 14*, 4953−4963.
40. Grathwohl, C., and Wüthrich, K. (1981) NMR studies of the rates of proline cis/trans isomerization in oligopeptides, *Biopolymers 20*, 2623−2633.
41. Reimer, U., Scherer, G., Drewello, M., Kruber, S., Schutkowski, M., and Fischer, G. (1998) Side-chain effects on peptidyl-prolyl cis/trans isomerization, *J. Mol. Biol. 279*, 449−460.
42. Stewart, D. E., Sarkar, A., and Wampler, J. E. (1990) Occurrence and role of cis peptide bonds in protein structures, *J. Mol. Biol. 269*, 611−622.
43. Schellman, J. A. (1955) The stability of hydrogen-bonded peptide structures in aqueous solution, *C. R. Trav. Lab. Carlsberg Ser. Chim. 29*, 230−259.
44. Matthews, B. W., Nicholson, H., and Becktel, W. J. (1987) Enhanced protein thermostability from site-directed mutations that decrease the entropy of unfolding, *Proc. Natl. Acad. Sci. U.S.A. 84*, 6663−6667.
45. Nemethy, G., Leach, S. J., and Scheraga, H. A. (1966) The influence of amino acid side chains on the free energy of helix−coil transitions, *J. Phys. Chem. 70*, 998−1004.
46. Yun, R. J., Anderson, A., and Hermans, J. (1991) Proline in α helix: stability and conformation studied by dynamics simulation, *Proteins 10*, 219−228.
47. Bechtel, W. J., and Schellman, J. A. (1987) Protein stability curves, *Biopolymers 26*, 1859−1877.
48. Lee, K. J., Xie, D., Freire, E., and Amzel, L. M. (1994) Estimation of changes in side-chain configurational entropy in binding and folding: general methods and application to helix formation, *Proteins 20*, 68−84.
49. Creamer, T. P. (2000) Side-chain conformational entropy in protein unfolded states, *Proteins 40*, 443−450.
50. Pickett, S. D., and Sternberg, M. J. E. (1993) Empirical scale of side-chain conformational entropy in protein folding, *J. Mol. Biol. 231*, 825−839.
51. Abagyan, R., and Totrov, M. (1994) Biased probability Monte Carlo conformational searches and electrostatic calculations for peptides and proteins, *J. Mol. Biol. 235*, 983−1002.
52. Donato, H., Jr., and Martin, R. B. (1974) Conformations of carp muscle calcium binding parvalbumin, *Biochemistry 13*, 4575−4579.
53. Haiech, J., Derancourt, J., Pechere, J.-F., and Demaille, J. G. (1979) Magnesium and calcium binding to parvalbumins: evidence for differences between parvalbumins and an explanation of their relaxing function, *Biochemistry 18*, 2752−2758.
54. Moeschler, H. J., Schaer, J.-J., and Cox, J. A. (1980) A thermodynamic analysis of the binding of calcium and magnesium ions to parvalbumin, *Eur. J. Biochem. 111*, 73−78.
55. Williams, T. C., Corson, D. C., Oikawa, K., McCubbin, W. D., Kay, C. M., and Sykes, B. D. (1986) ^{1}H NMR spectroscopic studies of calcium-binding proteins. 3. Solution conformations of rat apo-α-parvalbumin and metal-bound rat α-parvalbumin, *Biochemistry 25*, 1835−1846.
56. Permyakov, E. A., Medvedkin, V. N., Mitin, Y. V., and Kretsinger, R. H. (1991) Noncovalent complex between domain AB and domains CD*EF of parvalbumin, *Biochim. Biophys. Acta 1076*, 67−70.
57. Henzl, M. T., Shibasaki, O., Comegys, T. H., Thalmann, I., and Thalmann, R. (1997) Oncomodulin is abundant in the organ of Corti, *Heart Res. 106*, 105−111.
58. Sakaguchi, N., Henzl, M. T., Thalmann, I., Thalmann, R., and Schulte, B. A. (1998) Oncomodulin is expressed exclusively by outer hair cells in the organ of Corti, *J. Histochem. Cytochem. 46*, 29−39.
59. Zheng, J., Shen, W., He, D. Z., Long, K. B., Madison, L. D., and Dallos, P. (2000) Prestin is the motor protein of cochlear outer hair cells, *Nature 405*, 149−155.
60. Henzl, M. T., Serda, R. E., and Boschi, J. M. (1991) Identification of a novel parvalbumin in avian thymic tissue, *Biochem. Biophys. Res. Commun. 177*, 881−887.
61. Hapak, R. C., Stanley, C. M., and Henzl, M. T. (1996) Intrathymic distribution of the two avian thymic parvalbumins, *Exp. Cell Res. 222*, 234−245.
62. Heller, S., Bell, A. M., Denis, C. S., Choe, Y., and Hudspeth, A. J. (2002) Parvalbumin 3 is an abundant Ca^{2+} buffer in hair cells, *J. Assoc. Res. Otolaryngol 3*, 488−498.
63. Pack, A. K., and Slepecky, N. B. (1995) Cytoskeletal and calcium-binding proteins in the mammalian organ of Corti: cell type-specific proteins displaying longitudinal and radial gradients, *Heart Res. 91*, 119−135.

BI034721X